Signature of helium segregation in hydrogen-helium mixtures

Sebastien Hamel,[1] Miguel A. Morales,[1,2] and Eric Schwegler[1]
[1]*Lawrence Livermore National Laboratory*
[2]*Physics Department, University of Illinois at Urbana-Champaign, Urbana, Illinois, USA*
(Received 22 December 2010; revised manuscript received 19 July 2011; published 11 October 2011)

The conductivity and reflectivity of mixtures of hydrogen and helium under high pressure are calculated using first-principles molecular dynamics and the Kubo-Greenwood formula. Hydrogen-helium mixtures have been predicted to undergo demixing below a certain critical temperature. The impact of phase segregation of helium on the optical properties of the mixtures is explored. The change in reflectivity upon demixing is found to vary with frequency with larger variation at higher frequency.

DOI: 10.1103/PhysRevB.84.165110 PACS number(s): 78.15.+e, 78.20.Bh, 96.15.Nd, 96.30.Kf

I. INTRODUCTION

The lack of data from either direct observation or experiments leaves unanswered fundamental questions in planetary science. The hydrogen-helium mixtures account for most of the mass in giant planets, and so understanding their properties is crucial to advancing our understanding of the internal structure of these bodies. The use of theoretical data based on first-principles simulation of material properties to complement known data is an important development of recent planetary models.[1–5]

Recently, the thermodynamic properties of H-He mixtures were investigated using first-principles methods,[6,7] in particular the conditions under which the demixing of helium (sometimes referred to as helium rain) may occur. These studies predict that a large fraction of the interior of Saturn is in a regime where the hydrogen-helium mixture should phase separate. This phase separation provides an additional source of heat that may explain the planet's high luminosity considering its mass and age.[8,9] (Saturn and Jupiter are believed to have been formed approximately at the same time as the sun.) In order to verify this prediction, we need experimental confirmation of where the mixture will phase separate under extreme conditions. For now, the experimental evidence for this demixing is indirect, but the relevant conditions of temperature (thousands of Kelvin) and pressure (a few Mbar) may soon be achieved in using ramp-wave compression laser experiments. In this paper, based on first-principles calculations of electrical conductivity, we propose that reflectivity measurements carried out at high frequency will show a clear signature of the helium segregation.

II. METHOD

We used configurations drawn from first-principles molecular dynamics (FPMD) simulations of H-He mixtures at different temperatures and densities to investigate the impact of pressure, temperature, and helium concentration on the electrical (and thermal) conductivity of the mixtures. We considered four temperatures: 4, 6, 8, and 10 kK, nine helium concentrations (0%, 2%, 5%, 10%, 20%, 40%, 60%, 80%, and 100%), and densities corresponding to pressures ranging from 200 to 2000 GPa. For pure hydrogen, we also considered a lower density (0.37 g/m^3) at 10 kK, which is on the hydrogen principal Hugoniot, in order to validate our approach with previously published experimental and theoretical data.[10,11]

For each temperature and density, the electronic conductivity is evaluated on 15 well-spaced configurations drawn from the FPMD trajectory. The FPMD simulations performed in this work were based on Kohn-Sham density functional theory, using the Perdew-Burke-Ernzerhof (PBE) exchange-correlation functional. Empty states were included with an electronic temperature set to the ionic temperature. This electronic temperature is used to determine the (possibly fractional) occupation number of the orbitals according to a Fermi distribution. To integrate the equation of motion during the dynamics we used a time step of 8 a.u.

Most of the FPMD simulations were performed with the QBOX code. We used Born-Oppenheimer MD (BOMD) within the NVT ensemble (with a weakly coupled Berendsen thermostat), as implemented in the QBOX code (http://eslab.uc- davis.edu/software/qbox). We used a Hamann-type local pseudopotential with a core radius of $r_c = 0.3$ au to represent hydrogen and a Troullier-Martins-type nonlocal pseudopotential with s and p channels and $r_c = 1.091$ au to represent helium. A plane-wave energy cutoff of 90 Ry was used for $r_s < 1.10$ and of 115 Ry for $r_s > 1.10$. We used 250 electrons. The Brillouin zone was sampled at the Γ point. To reduce systematic effects and to get accurate pressures, we added a correction to the EOS designed to correct for the plane-wave cutoff and the sampling of the Brillouin zone. To compute this, we studied 15–20 configurations at each density and composition by using a $4 \times 4 \times 4$ grid of k points with a plane-wave cutoff of at least 300 Ry. The actual plane-wave cutoff used depended on density and was chosen to achieve full convergence in the energy and pressure. Averages were accumulated for at least 2000 time steps after having first equilibrated the system, using a suitable effective model and subsequently allowed 300–500 time steps of equilibration with DFT.

Additional simulations performed in this work, including conductivity calculations as well as FPMD simulations of metastable mixtures reported below, were performed with the Vienna *ab initio* Simulation Package (VASP).[12] VASP and QBOX use different pseudopotentials, and we verified that pressures were consistent when large plane-wave energy cutoffs were used. The VASP simulations are also performed at the PBE[13] level of approximation to the exchange-correlation functional with projector-augmented wave (PAW)[14]

pseudopotentials to account for the core electrons.[15] The additional simulations of the phase-separated system performed with VASP used 250 hydrogen atoms and 167 helium atoms to reach a concentration of 40% He.

For each configuration drawn from the trajectories, we used the gamma point electronic density from the MD to evaluate the set of Kohn-Sham orbitals at the $(\frac{1}{4},\frac{1}{4},\frac{1}{4})$ k point (again using Fermi broadening at the ionic temperature). Based on these orbitals,[16] we use the Kubo-Greenwood formula to estimate the real component of the frequency-dependent conductivity:[11,17,18]

$$\sigma(\omega) = \frac{2\pi e^2\hbar^2}{3m^2\omega\Omega}\sum_{\mathbf{k}} W(\mathbf{k}) \sum_{j=1}^{N}\sum_{i=1}^{N}\sum_{\alpha=1}^{3}[F(\epsilon_{i,\mathbf{k}}) - F(\epsilon_{j,\mathbf{k}})] \times |\langle\Psi_{j,\mathbf{k}}|\nabla_\alpha|\Psi_{i,\mathbf{k}}\rangle|^2\delta(\epsilon_{i,\mathbf{k}} - \epsilon_{j,\mathbf{k}} - \hbar\omega), \quad (1)$$

where e and m are the electron charge and mass, Ω the cell volume, α denotes the x, y, and z directions, and $F(\epsilon_{i,\mathbf{k}})$ is the occupation number. The sum over k points is performed using only the $(\frac{1}{4},\frac{1}{4},\frac{1}{4})$ k point. This approximation was validated using a $4\times4\times4$ grid of k points for a few configurations. The change in the DC conductivity with configurations was found to be much larger that the change due to k-point sampling, which was at most a few percent. The dc conductivity is obtained as the zero frequency limit of $\sigma(\omega)$ averaged over the different configurations, while the imaginary component of the conductivity is obtained by using the Kramers-Kronig transform:

$$\sigma_2(\omega) = -\frac{2}{\pi}P\int_0^\infty \frac{\sigma(\nu)\omega}{(\nu^2-\omega^2)}\,d\nu, \quad (2)$$

where P denotes the principal value of the integral. Using the complex conductivity, we can get the complex dielectric function ϵ, the index of refraction n, the coefficient of extinction k, and the reflectivity R:

$$\epsilon_1(\omega) = 1 - \frac{4\pi}{\omega}\sigma_2(\omega); \quad \epsilon_2(\omega) = \frac{4\pi}{\omega}\sigma(\omega), \quad (3)$$

$$\epsilon(\omega) = \epsilon_1(\omega) + i\epsilon_2(\omega) = [n(\omega) + ik(\omega)]^2, \quad (4)$$

$$R(\omega) = \frac{[1-n(\omega)]^2 + k^2(\omega)}{[1+n(\omega)]^2 + k^2(\omega)}. \quad (5)$$

III. RESULTS AND DISCUSSION

A. Hydrogen

In Fig. 1 we plot the frequency-dependent electronic conductivity obtained using Eq. (1) for hydrogen along a isotherm of 10 000 K for densities ranging from low-density (LD) 0.37 g/cm^3 to high-density (HD) 2.33 g/cm^3. The frequency dependence of the conductivity of hydrogen shows a peak at zero photon energy for all densities except the lowest, which has a peak at finite photon energy. This change in shape of the frequency dependence has importance consequences for the reflectivity, which is 0.5 for this 0.37 g/cm^3 point, while it is 0.7–0.8 for the higher densities. This and a relatively low dc conductivity of hydrogen at a density of 0.37 g/cm^3 are the result of a pseudogap forming in the DOS. This change from a metal at HD to a semimetal at LD can be seen in the Electron

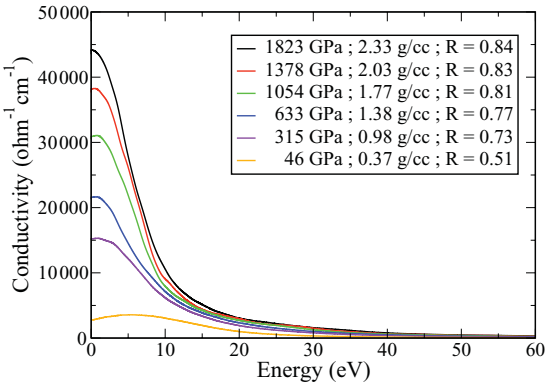

FIG. 1. (Color online) Frequency-dependent electronic conductivity of hydrogen at 10 000 K for densities ranging from 0.37 to 2.33 g/cm^3. The corresponding reflectivity at 1064 nm is included in the legend.

Localization Function (ELF)[19] reported in Fig. 2. The volume enclosed by the silver isosurface (ELF = 0.5: homogeneous electron gas-like) but not the red one (ELF = 0.75: more localized) is much larger for the HD hydrogen, pointing to a more delocalized charge density. For the LD hydrogen the ELF show a high degree of localization around pairs of hydrogen atoms.

B. Hydrogen-helium mixtures

For the densities and temperatures considered here, pure helium exhibits a large band gap. At the highest density (4.62 g/cm^3) and temperature (10 000 K) calculated, we obtained an average gap of 9.5 eV. At the lowest density (1.95 g/cm^3) and temperature (4000 K), the gap increases to 13.8 eV. Even with these large gaps, the temperature broadening of the Fermi distribution allows for some small occupation of the conduction bands leading to a small conductivity (1–10 ohm^{-1} cm^{-1}) for helium. This is to be compared with conductivities in the tens of thousands ohm^{-1} cm^{-1} for hydrogen under similar density and temperature conditions. Hence, for all the H-He mixtures calculated in this work the dc conductivity is essentially coming from the hydrogen component of the fluid. For all the concentrations, the dc conductivity was found to increase approximately linearly with pressure and decrease exponentially with the concentration of

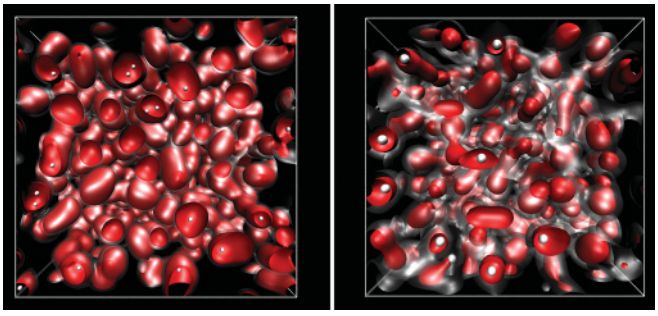

FIG. 2. (Color online) ELF of hydrogen at 10 000K for densities of 0.37 and 2.33 g/cm^3. The silver isosurface is for a value of 0.5 (homogeneous electron gas-like), and the red is for 0.75 (more localized). The white spheres denote the hydrogen atoms and have the same absolute size to illustrate the change in density.

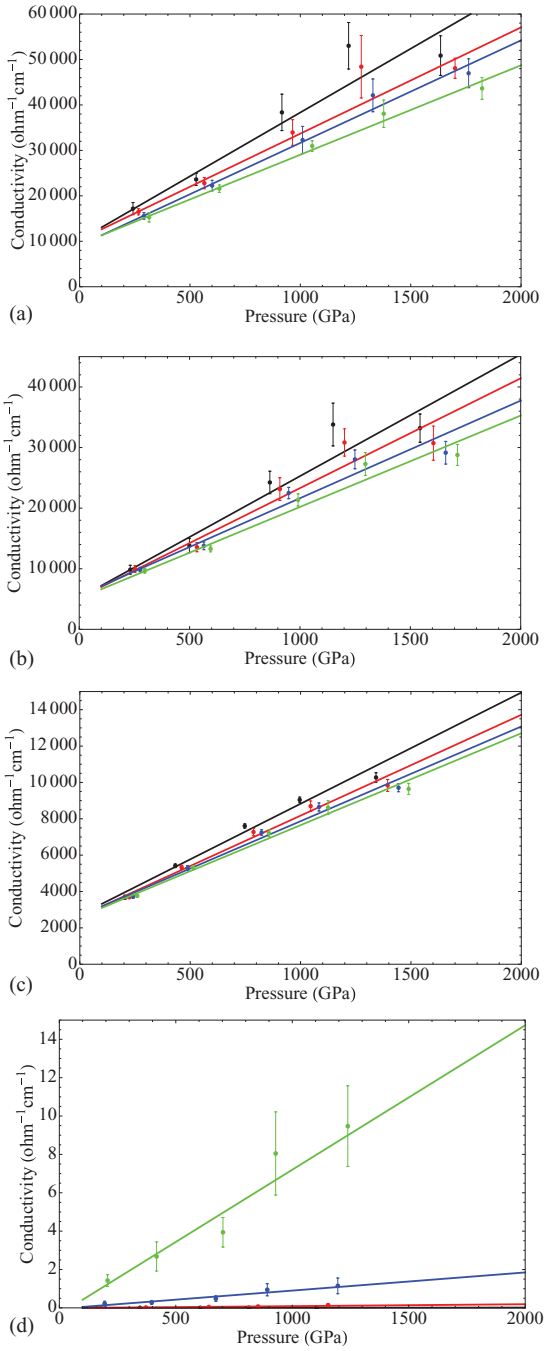

FIG. 3. (Color online) DC conductivity vs pressure for 4 kK (black), 6 kK (red), 8 kK (blue), and 10 kK (green): (a) Pure hydrogen, (b) H-He mixture with 10% helium, (c) H-He mixture with 40% helium, (d) pure helium. The standard deviation over the different configurations is used as an estimate of the uncertainty. For this system, this uncertainty is larger than the error coming from size effects or from an incomplete sampling of k space.

helium. Compared to the impact of helium concentration and pressure on the dc conductivity, the impact of temperature is rather small in the range considered here but tends to decrease the dc conductivity (Fig. 3, Tables I–IV). The only exception to this is pure helium, where, because of the presence of a gap, the conductivity increases with temperature.

TABLE I. DC conductivity of H-He mixtures at 4 kK.

X	Density (g/cm^3)	P (GPa)	σ_{DC} (S/cm)	$\Delta\sigma_{DC}$ (S/cm)
0	0.98	241.9	17190	1332
0	1.38	528	23610	1299
0	1.77	916.5	38365	4012
0	2.03	1218.7	53017	5115
0	2.33	1635.4	50856	4355
0.02	1.01	239.7	15213	853
0.02	1.42	522.4	21341	1833
0.02	1.83	905.8	34762	1682
0.1	1.15	231.4	9848	725
0.1	1.62	499.1	13811	1169
0.1	2.08	863.6	24242	1859
0.1	2.38	1150	33798	3531
0.1	2.73	1544.1	33207	2330
0.2	1.31	220.2	6244	364
0.2	1.84	471.8	8670	288
0.2	2.36	817.3	16223	849
0.2	2.70	1087.5	20681	2168
0.2	3.10	1463.7	19510	1060
0.4	1.53	203.9	3682	116
0.4	2.15	432.4	5414	101
0.4	2.77	747.2	7604	116
0.4	3.16	996.1	9039	155
0.4	3.63	1341.8	10275	256
1	1.95	160.3	0	0
1	2.74	345.8	0	0
1	3.52	605.2	0	0
1	4.02	813.5	0	0
1	4.62	1105.9	0	0

For the 10 000 K isotherm, we obtained a good fit ($R^2 = 0.999$) of the dc conductivity using

$$\begin{aligned} \sigma_{\mathrm{HHe}}(P,X) &= -0.23 + 9201.41 b_1(X) + 19.6767 b_2(X) P, \\ b_1(X) &= e^{-5.62559X - 1.07678X^2 - 9.69242X^{12}}, \\ b_2(X) &= e^{-2.77475X - 0.457604X^2 - 4.40873X^5}, \end{aligned} \tag{6}$$

where P is the pressure in GPa, $X = \frac{N_{\mathrm{He}}}{N_{\mathrm{H}}+N_{\mathrm{He}}}$ is the helium concentration, and σ is in units of ohm^{-1} cm^{-1} (see Fig. 4). The fit was constructed first by using a linear function for the pressure dependence and then fitting the concentration dependence of the slopes and intercepts. For the pressure dependence fit, the standard deviation of the conductivity was used as a measure of uncertainty [i.e., the conductivity values are weighted by $1/(\Delta\sigma)^2$]. There appears to be a plateau of conductivity reached at higher pressure and lower temperature for pure hydrogen as well as mixtures with low concentration of helium. Hence, the linear regression may not be the best choice, but considering the errors bars (given by the standard deviation of the snapshots), going beyond a linear fit is not warranted at this time. This possible plateau will need to be investigated at higher pressure. We note that this functional form used for $\sigma_{\mathrm{HHe}}(P,X)$ interpolates smoothly the FPMD data but may not be reliable outside the calculated range of densities.

TABLE II. DC conductivity of H-He mixtures at 6 kK.

X	Density (g/cm^3)	P (GPa)	σ_{DC} (S/cm)	$\Delta\sigma_{DC}$ (S/cm)
0	0.98	267	16496	682
0	1.38	565.1	22790	1226
0	1.77	964.8	33942	2809
0	2.03	1276.1	48410	6871
0	2.33	1701	48070	2211
0.02	1.01	264.4	14978	871
0.02	1.42	560.2	19993	1528
0.02	1.83	953.8	31600	1833
0.1	1.15	253.3	9980	537
0.1	1.62	533.3	13563	761
0.1	2.08	908.9	23149	1871
0.1	2.38	1201.8	30836	2238
0.1	2.73	1604.6	30726	2809
0.2	1.31	241.7	6148	270
0.2	1.84	503.5	8943	470
0.2	2.36	857.9	15491	1390
0.2	2.70	1138	19231	1454
0.2	3.10	1518.9	18613	1260
0.4	1.53	223.7	3693	85
0.4	2.15	461.2	5331	113
0.4	2.77	786.7	7271	198
0.4	3.16	1045.6	8697	283
0.4	3.63	1394.5	9834	327
1	1.95	178.9	0	0
1	2.74	372	0	0
1	3.52	641.8	0	0
1	4.02	853.4	0	0
1	4.62	1153.9	0	0

With mixtures, it is often practical to consider mixing models in order to interpolate between the pure components. One of these models is the pressure-matching linear mixing model (PMLM)[18] defined as

$$\sigma_{\mathrm{HHe}}^{\mathrm{PMLM}}(P,X) = \left[\frac{V_{\mathrm{H}}(P)}{V_{\mathrm{HHe}}(P,X)}\right]\sigma_{\mathrm{H}}(P) + \left[\frac{V_{\mathrm{He}}(P)}{V_{\mathrm{HHe}}(P,X)}\right]\sigma_{\mathrm{He}}(P), \quad (7)$$

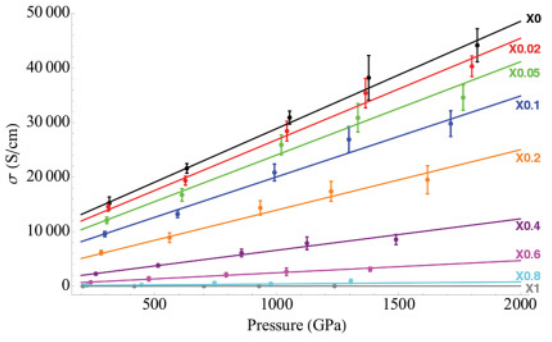

FIG. 4. (Color online) The symbols are the FPMD dc conductivity with error bar taken from the standard deviation between configurations. The lines are from a fit to the FPMD dc conductivities using Eq. (6). The temperature is 10 000 K.

TABLE III. DC conductivity of H-He mixtures at 8 kK.

X	Density (g/cm^3)	P (GPa)	σ_{DC} (S/cm)	$\Delta\sigma_{DC}$ (S/cm)
0	0.98	291.6	15603	720
0	1.38	600.4	22259	1164
0	1.77	1010.1	32282	3003
0	2.03	1328.8	42109	3609
0	2.33	1762.4	46969	3175
0.02	1.01	289.4	14622	672
0.02	1.42	594.8	19628	723
0.02	1.83	998.8	29713	2080
0.02	2.09	1314.9	37884	2849
0.02	2.40	1742.3	42006	2249
0.05	1.08	282.8	12224	507
0.05	1.51	581.3	16543	713
0.05	1.94	978	25822	1422
0.05	2.22	1285.3	33117	2176
0.05	2.55	1707.4	35367	2405
0.1	1.15	276	9858	373
0.1	1.62	564.6	13772	634
0.1	2.08	948.9	22495	939
0.1	2.38	1249	28047	1559
0.1	2.73	1660.3	29147	1869
0.2	1.31	262.3	6215	293
0.2	1.84	533.1	8886	290
0.2	2.36	896.1	14650	857
0.2	2.70	1181	18779	1234
0.2	3.10	1570.7	19577	1172
0.4	1.53	241.3	3728	97
0.4	2.15	488.4	5289	140
0.4	2.77	823.4	7244	154
0.4	3.16	1083.5	8651	223
0.4	3.63	1443.8	9708	219
1	1.95	194.6	0	0
1	2.74	396.5	0	0
1	3.52	672.1	0	0
1	4.02	892.7	1	0
1	4.62	1195.5	1	0

where

$$V_{\mathrm{HHe}}(P,X) = (1-X)V_{\mathrm{H}}(P) + XV_{\mathrm{He}}(P). \quad (8)$$

Here we consider this linear mixing model for two reasons. First, our explicit simulation of mixtures of helium and hydrogen of different concentration can be used to access the quality of the PMLM model for the dc conductivity and for the equation of state of the mixture.

Second, the PMLM model describes a system where two components are completely isolated from each other but at equivalent temperature and pressure (it is a mixing of noninteracting species). When the two components are homogeneously mixed, this is always an approximation to the real system. But when the two components are phase separated but remain in mechanical equilibrium (i.e., they have the same pressure and temperatures), this model becomes a very good approximation of the real system. In fact, in this case, the

TABLE IV. DC conductivity of H-He mixtures at 10 kK.

X	Density (g/cm^3)	P (GPa)	σ_{DC} (S/cm)	$\Delta\sigma_{DC}$ (S/cm)
0	0.98	315	15265	1022
0	1.38	633.2	21579	823
0	1.77	1053.8	30972	1156
0	2.03	1377.7	38064	3011
0	2.33	1823.3	43639	2402
0.02	1.01	310.5	14524	689
0.02	1.42	627.3	19381	936
0.02	1.83	1043	28328	1234
0.02	2.09	1364.5	35242	2441
0.02	2.40	1801.4	40624	2005
0.05	1.08	305.4	12023	442
0.05	1.51	613.2	16540	662
0.05	1.94	1019.8	25925	1551
0.05	2.22	1334.3	31414	2061
0.05	2.55	1765.2	34052	1097
0.1	1.15	297	9675	387
0.1	1.62	595	13283	494
0.1	2.08	991.6	21352	1001
0.1	2.38	1296.5	27284	1879
0.1	2.73	1713.5	28772	1721
0.2	1.31	282	6485	265
0.2	1.84	562.2	8982	493
0.2	2.36	934.2	14387	894
0.2	2.70	1224	17964	1280
0.2	3.10	1619.4	19355	1101
0.4	1.53	260	3765	76
0.4	2.15	514.7	5315	111
0.4	2.77	856.7	7208	194
0.4	3.16	1124.6	8619	377
0.4	3.63	1489.7	9642	309
0.6	1.71	238.887	714	168
0.6	2.40	477.353	1337	374
0.6	3.09	794.106	2089	371
0.6	3.53	1041	2661	693
0.6	4.06	1384.34	3094	365
0.8	1.84	224.014	154	88
0.8	2.59	447.027	229	103
0.8	3.32	745.506	546	272
0.8	3.80	977.054	410	243
0.8	4.37	1304.88	876	372
1	1.95	207.1	1	0
1	2.74	417.5	3	1
1	3.52	702.5	4	1
1	4.02	928.8	8	2
1	4.62	1238.4	9	2

PMLM model is an approximation only in that the impact of the interface on the transport properties is neglected.

A good fit ($R^2 = 0.998$) of the FPMD pressure-temperature-density data from which we can evaluate the volume fractions in the linear mixing model is given by

$$\rho = \{a_{\mathrm{H}}(T) + [a_{\mathrm{He}}(T) - a_{\mathrm{H}}(T)]X\}P^{c(T)}, \quad (9)$$

where X is the concentration in He. As a function of temperature, the parameters are given by

$$a_{\mathrm{H}}(T) = 0.109651 - 7.07335\times10^{-6}T + 2.37907\times10^{-10}T^2,$$
$$a_{\mathrm{He}}(T) = 0.247818 - 1.57444\times10^{-5}T + 5.33961\times10^{-10}T^2,$$
$$\mathrm{c}(T) = 0.422708 + 9.48002\times10^{-6}T - 2.6347\times10^{-10}T^2,$$

with densities given in (g/cm^3), temperatures in Kelvin and pressures in GPa.

For a mixture with 40% helium at 1500 GPa, the calculated conductivity is four times smaller than for pure hydrogen at the same pressure. By comparison, a PMLM model based on pure helium and pure hydrogen would predict only a factor of two reduction in conductivity. This also means that if the conditions are such that the H-He system segregates into a pure He fraction and a pure H fraction under constant pressures (reaching a state well described by a linear mixing rule), the overall

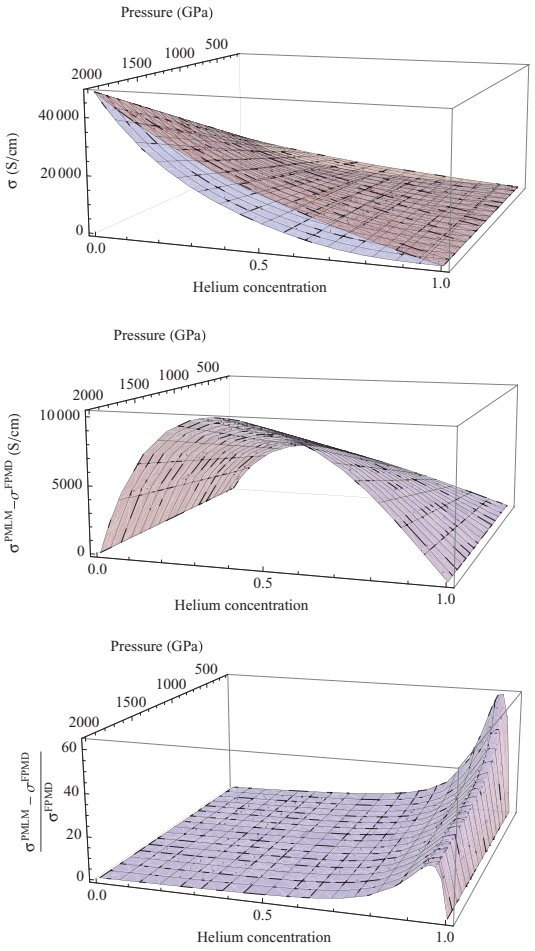

FIG. 5. (Color online) (Top) The dc conductivity of the H-He mixture given by PMLM model (pink) and calculated with FPMD (blue). (Middle) Difference between the PMLM model and FPMD dc conductivity. The PMLM model corresponds to the conductivity the completely demixed fluid. (Bottom) The relative difference $\frac{\sigma^{\mathrm{PMLM}}-\sigma^{\mathrm{FPMD}}}{\sigma^{\mathrm{FPMD}}}$ exhibits the largest difference at high helium concentration.

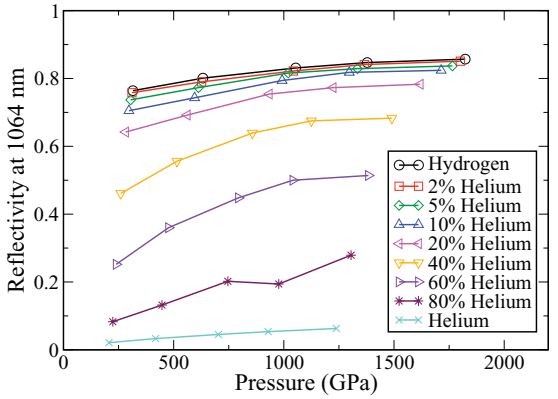

FIG. 6. (Color online) Reflectivity at 1064 nm as a function of pressure and helium concentration at a temperature of 10 000 K.

conductivity will increase dramatically. Such a demixing of helium in metallic hydrogen is predicted for Saturn (and to a lesser extend in Jupiter).[6,7] Note that the increase is particularly important for higher helium concentration (Fig. 5).

Whilethe dc conductivity is a crucial quantity for magnetic fields and thermal profile model of planets, the quantity that is most relevant for laser-driven shock-compression experiments is the reflectivity. This is what is measured with the use of VISAR diagnostics.[20,21] In Fig. 6 we show the FPMD reflectivity at a frequency of 1064 nm as a function of pressure and helium concentration for the 10 000 K isotherm. As for the DC conductivity, the reflectivity of H-He mixtures increases with pressure and decreases with helium concentration.

In order to investigate the impact of helium segregation on the reflectivity, we prepared a (40% He) mixture in both the mixed and segregated phases, as well as the pure states under 1500 GPa and 10 000 K conditions. The segregated phase is a metastable system that was prepared by first fixing the cross section of a pure H and a pure He and varying the length of the boxes to reach the target pressure. Once the pure systems are equilibrated, the boxes are brought in contact with each other, and the stress at the interfaces is relieved by running MD on each subsystem, freezing the atomic position of the other subsystem. Then the volume is fixed, and a MD is continued with all the atoms free to move. Under this large pressure, very little diffusion was observed at this point. Configurations from this MD were drawn (Fig. 7), and we evaluated the conductivity using Eq. (1) in the direction along the slab. This arrangement comes very close to a pressure-matching linear mixing (the only difference is in the "thickness" of the interface).

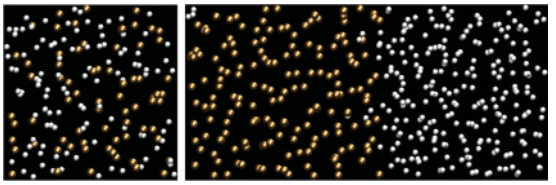

FIG. 7. (Color online) 40% He mixtures at 10 000 K, 1500 GPa, and average density 3.63 g/cm^3: (a) mixed phase, (b) segregated in "slabs" with the conductivity calculated along the slab.

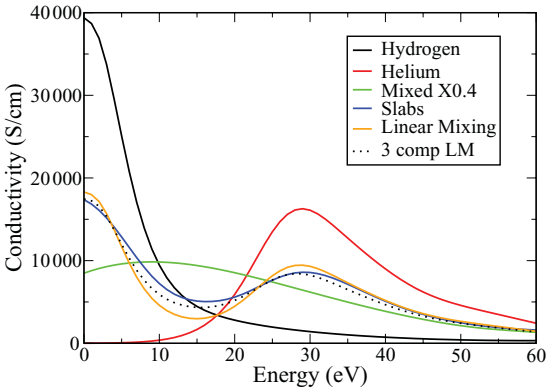

FIG. 8. (Color online) Signature of He segregation in the frequency dependence of the conductivity.

The frequency-dependent conductivity $\sigma(\omega)$ for pure H, pure He, the 40% He mixture (mixed and segregated) as well as the prediction of the pressure-matching LM model are shown in Fig. 8. One can clearly see the very different features of the pure hydrogen and pure helium system with the latter's onset of conductivity around ∼10 eV photon energy (gap energy). As they should, these features (H peak at 0 eV and He peak at 30 eV) are also seen in the LM model and in the "slab" $\sigma(\omega)$, which is very close to the LM model, but are completely missing from the fully mixed system. Under these P-T conditions, the pure H and pure He spectra have a isosbectic point at 17.675 eV, and any mixing models based only on the pure references are bound to pass through that point. That the mixed system does not pass through that point is clear evidence of an electronically different fluid from either of its components. Using a three-component LM model that includes the mixed spectra, we can estimate the volume fraction (∼20%) needed to reproduce the slab calculation and obtain an interface "thickness" of ∼1.2 Å.

Using Eq. (5), we evaluate the frequency-dependent reflectivity. As noted above, even though at very low frequency the mixed 40% He system has half the conductivity of the segregated system and a quarter of that of pure hydrogen, the low-frequency part of the reflectivity of these systems is similar. Only with increasing photon energy do the reflectivities diverge from one another (Fig. 9). Even though the difference

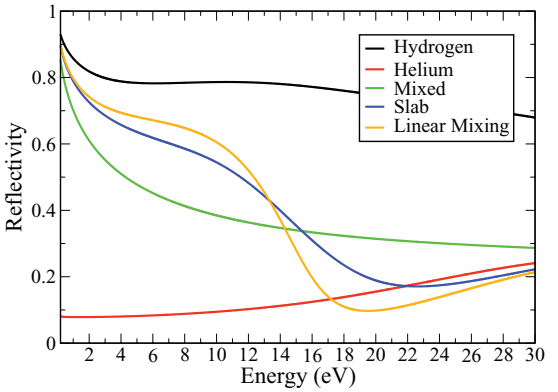

FIG. 9. (Color online) Signature of He segregation in the frequency dependence of the reflectivity.

TABLE V. Reflectivity for H-He mixtures at 10 000 K, 1500 GPa.

λ (nm)	energy (eV)	H	He	×0.4 Mixed	LM	×0.4 slab
1064	1.166	0.83	0.08	0.64	0.76	0.74
532	2.335	0.81	0.08	0.59	0.73	0.71
350	3.545	0.79	0.08	0.53	0.70	0.67
248.25	5.0	0.78	0.08	0.48	0.68	0.64
124.125	10.0	0.79	0.09	0.38	0.61	0.54

between mixed and segregated is obvious around 10 eV, the separation is significant around 3 eV. We report values for some laser frequency used in VISAR diagnostics in Table V. We propose that measuring an increase in reflectivity under constant pressure (and temperature) conditions may be the signature of the demixing of helium from the H-He mixture. Using a multichannel VISAR to identify a larger effect at higher frequency would be further indication that demixing is observed.

ACKNOWLEDGMENT

This work was performed under the auspices of the U.S. Department of Energy under contract DE-AC52-07NA27344.

[1] J. J. Fortney and W. B. Hubbard, Icarus **164**, 228 (2003).
[2] J. J. Fortney and W. B. Hubbard, Astrophys. J. **608**, 1039 (2004).
[3] J. J. Fortney and N. Nettelmann, Space Sci. Rev. **152**, 423 (2010).
[4] N. Nettelmann, B. Holst, A. Kietzmann, M. French, R. Redmer, and D. Blaschke, Astrophys. J. **683**, 1217 (2008).
[5] J. Vorberger, I. Tamblyn, B. Militzer, and S. A. Bonev, Phys. Rev. B **75**, 024206 (2007).
[6] M. A. Morales, E. Schwegler, D. M. Ceperley, C. Pierleoni, S. Hamel, and K. Caspersen, Proc. Natl. Acad. Sci. USA **106**, 1324 (2009).
[7] W. Lorenzen, B. Holst, and R. Redmer, Phys. Rev. Lett. **102**, 115701 (2009).
[8] D. J. Stevenson and E. E. Salpeter, Astrophys. J. Suppl. Ser. **35**, 221 (1977).
[9] D. J. Stevenson and E. E. Salpeter, Astrophys. J. Suppl. Ser. **35**, 239 (1977).
[10] P. M. Celliers, G. W. Collins, L. B. DaSilva, D. M. Gold, R. Cauble, R. J. Wallace, M. E. Foord, and B. A. Hammel, Phys. Rev. Lett. **84**, 5564 (2000).
[11] B. Holst, R. Redmer, and M. P. Desjarlais, Phys. Rev. B **77**, 184201 (2008).
[12] G. Kresse and J. Hafner, Phys. Rev. B **47**, 558 (1993); **49**, 14251 (1994); G. Kresse and J. Furthmüller, Comput. Mater. Sci. **6**, 15 (1996); Phys. Rev. B **54**, 11169 (1996).
[13] J. P. Perdew, K. Burke, and M. Ernzerhof, Phys. Rev. Lett. **77**, 3865 (1996); **78**, 1396 (1997).
[14] P. E. Blöchl, Phys. Rev. B **50**, 17953 (1994); G. Kresse and D. Joubert, *ibid*. **59**, 1758 (1999).
[15] We used a plane-wave energy cutoff of 500 eV for the conductivity calculations. A few configurations were tested with a 1200 eV cutoff to verify that spectra were well converged with respect to plane-wave energy cutoff.
[16] In the conductivity calculation, we use a sufficient amount of unoccupied orbitals to capture all excitations below 60 eV. This allowed us to verify that the Kramers-Kronig transform was converged for the frequency interval considered here.
[17] T. R. Mattsson and M. P. Desjarlais, Phys. Rev. Lett. **97**, 017801 (2006).
[18] D. A. Horner, J. D. Kress, and L. A. Collins, Phys. Rev. B **77**, 064102 (2008).
[19] A. D. Becke and K. E. Edgecombe, J. Chem. Phys. **92**, 5397 (1990); B. Silvi and A. Savin, Nature (London) **371**, 683 (1994).
[20] D. G. Hicks, T. R. Boehly, P. M. Celliers, J. H. Eggert, S. J. Moon, D. D. Meyerhofer, and G. W. Collins, Phys. Rev. B **79**, 014112 (2009).
[21] P. M. Celliers, G. W. Collins, L. B. Da Silva, D. M. Gold, and R. Cauble, Appl. Phys. Lett. **73**, 1320 (1998).